

# Predictive Surveillance Technique for Air-Launched Rocket Motors

G. J. Svob\*

*Aerojet Tactical Systems Company, Sacramento, California*  
and

K. W. Bills Jr.†

*Aerojet Strategic Propulsion Company, Sacramento, California*

This paper discusses progress on a program designed to assess the feasibility of a new predictive surveillance concept for small air-launched rocket motors. The concept involves chemical/structural overtesting of aged full-scale motors in sufficient numbers to permit statistical treatment of the data and extrapolations to motor age-out. Key elements of the approach include the formulation of a practical overtest cycle, which will produce structural failures in a reasonable and predictable time, tests to failure of motors from selected age groups, and, finally, statistical evaluation of the resulting data to permit predictions of the remaining useful life. Results from the application of this technique to a typical air-launched motor are presented.

## Introduction

SOLID propellant rocket motors generally reach the end of useful life when structural or ballistic capabilities of the propellant-liner-insulation system are no longer adequate to meet structural requirements or performance specifications. The failure mode, which ultimately becomes life-limiting, depends upon the initial design safety margins and how these margins are altered by the combined effects of chemical and mechanical aging which occur during motor deployment. Although service life estimates, based on propellant and bond accelerated aging studies, are made during most tactical motor development efforts, the large uncertainties associated with motor environmental histories and the complex interactions between chemical aging and mechanical damage combine to make these preliminary estimates highly inaccurate and of little practical use in predicting motor age-out.

Motor ballistic parameters are generally quite insensitive to aging-induced structural changes, short of an actual failure such as grain cracking or bond separation. Because of this, current approaches to air-launched motor surveillance, i.e., annual static firings of motors selected from the operational inventory provide valid status information, but no data which are helpful in making a projection to that point in time when the motors will no longer be serviceable.

Fortunately, when dealing with small, air-launched motors it is reasonable to consider chemical/structural overtesting of full-scale aged motors in sufficient numbers to permit statistical treatment of the data and extrapolations to motor age-out. The major premise in this concept is that motor structural capabilities are degraded measurably (in a statistical sense) as the motors age. Successful use of this approach will therefore depend upon several key factors: 1) ability to fail the motors structurally with a reasonable overtest cycle; 2) motor selection to ensure a representative sample; 3) sufficient age spread between motor sets; and 4) sufficient number of motors in each set.

The subject program was designed to evaluate the feasibility of utilizing this concept for predicting the

remaining life of air-launched motors by demonstrating its application to a currently operational air-launched motor. The purpose of this paper is to describe the specific approach taken, summarize the results obtained, and assess the general applicability of the concept.

First, inspection of these data show that the motor-to-motor variability is very large at all motor ages, actually exceeding the range of ordinary statistical variations. Because of this large variability, the aging trends indicated for the data are not statistically significant. Second, the elongation data show a significant reduction from the original, but no apparent change between 4 and 143 months of age. This is suggestive of an initial bias between the Q.A. sample and motor grain.

## Dissected Motor

One of the unaged groups of motors was dissected to provide samples for a complete mechanical properties characterization. In addition, gradients across the web of the grain were evaluated using mini-tensile specimens tested at constant rate.

A comparison of test values from the motor with those obtained from the initial Q.A. carton sample for the same batch is presented in Table 2. Consistent with experience with other motors the bias takes the form of increased modulus ( $E_0$ ) and reduced elongation ( $\epsilon_m$ ) for the motor. Tensile strengths ( $\sigma_m$ ) are quite similar. It should be noted that the elongation reduction observed here is consistent in magnitude with that shown earlier in the discussion of the excised sample results.

The mini-tensile profiles for the grain, illustrated in Fig. 3, show significant variations with the general tendency being increasing hardness with increasing distance from the motor axis. Specimen orientation (hoop or axial) appeared to have little effect on the results. Of most significance is the observation that the propellant in the critical slot area appears to be harder than that in the lower stress regions.

## Grain Stress Analysis

Using the mechanical properties data obtained from the dissected motor as primary input, a stress analysis was performed to determine the minimum margin conditions, and thereby confirm the most likely failure mode. To account for the gradients shown in Fig. 3, the axisymmetric portion of the grain was divided into three layers with the relaxation

Presented as Paper 82-1097 at the AIAA/SAE/ASME 18th Joint Propulsion Conference, Cleveland, Ohio, June 21-23, 1982; submitted June 25, 1982; revision received Aug. 3, 1983. Copyright © American Institute of Aeronautics and Astronautics, Inc., 1983. All rights reserved.

\*Engineering Manager, Propellant Research and Development.

†Associate Scientist, Chemical Research and Development.

modulus of each adjusted to be consistent with the observed modulus profile.

The results of the analysis, summarized in Table 3, show that the minimum margin is associated with the inner bore strain for the condition of low-temperature storage. It was noted, however, that at the lowest temperatures the bond normal stress margin was also quite low, so at this stage bond separation could not be ruled out completely as a possible failure mode.

#### Overtest Cycle Selection

After considering a number of potential overtest cycles, it was determined that a simple shock cycle between temperature extremes would be the most effective in terms of producing the level of damage required to fail the motors in a reasonable time. Preliminary design curves for selecting the specific temperatures to be used were generated from calculations made using the Navy's Structural Design Nomograph.<sup>1</sup> As shown in Fig. 4, these curves yield predictions of the number of shock thermal cycles required to produce bore failures for various temperature exposures.

This nomographic procedure offers a specific advantage over other failure analyses in that it contains a "calibration" step to correct the predictions in terms of available strain evaluation cylinder (SEC) failure observations. The only available, low-temperature, SEC failure data were obtained from SEC's stepwise cooled to failure. Since this is a less damaging condition than shock thermal cycling, several thermoviscoelastic/damage analyses were conducted to provide conversions for the SEC data to give equivalent damage for thermal cycling.

#### Technical Approach

The overall approach to the subject program is illustrated by the logic flow diagram presented in Fig. 1. As indicated, the program is divided into three phases.

Phase I involved the development and demonstration of a practical test cycle which would accelerate in a predictable fashion the aging/damage rates in the critical grain locations, and produce failure within a reasonable time frame.

The key to success in phase I was an accurate cumulative damage analysis of the most likely failure locations in the grain. The results of this analysis were quite sensitive to, and could be no better than, the input information. Since the material properties are the most important unknowns in this category, it was felt that excised sampling of all of the motors plus the dissection and testing of one motor early in phase I was imperative. This motor, selected from the youngest group, provided the response and failure properties needed for the structural margin assessment, as well as the input parameters required for the calculation of damage rates.

Using the above data a detailed structural analysis was conducted and safety margins evaluated. Those areas/conditions giving the minimum margins then provided the focus for subsequent cumulative damage analyses of potential test cycles. Based on the results of the cumulative damage analysis, a test cycle was selected for validation through motor testing. Successful completion of the latter showed the cycle to be operative and ready for application in phase II.

In phase II three groups of full-scale motors, selected according to age, were simultaneously subjected to the validated test cycle. Cycling continued until half of the motors in each age group failed. The surviving motors from each group were then statically fired at low temperature.

Phase III of the program was designed to provide the final analytical determinations that lead to predictions of motor age-out, from either ballistic or structural causes. Extreme value statistical procedures were used in making these projections to determine the expected "first failures" of the missile inventory. Upon completion of these analyses, the overall concept of predictive surveillance techniques and this

experimental application of it were reassessed to determine their general applicability and provide recommendations for future work.

## Results and Discussion

#### Motor Description

The motor selected for the demonstration of the subject predictive surveillance concept is quite conventional in design featuring a five-pointed star grain perforation and utilizing a propellant containing 86% solids in a carboxy-terminated polybutadiene binder. The grain is about 8 in. in diameter and 42 in. long and is fully bonded along the cylindrical surface.

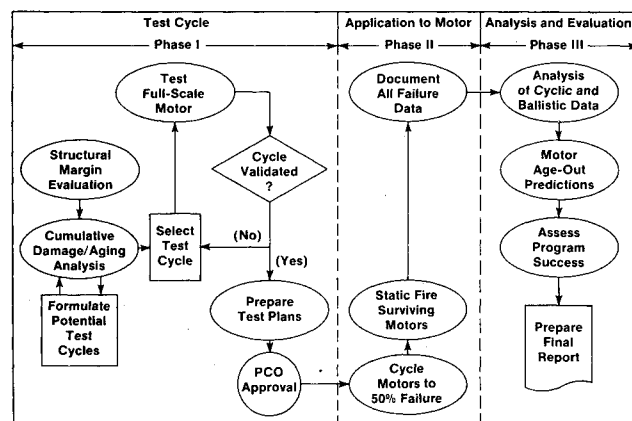


Fig. 1 Overall logic flow for predictive surveillance program.

Table 1 Motor vital statistics

Motor	Lot	Shipped from	Age at test, months
SN 0293	SP-406	HPC, McGregor	4
SN 0321	SP-406	HPC, McGregor	4
SN 0323	SP-406	HPC, McGregor	4
SN 0331	SP-406	HPC, McGregor	4
SN 0333	SP-406	HPC, McGregor	4
SN 5328	SP-271	England	109
SN 5081	SP-285	California	114
SN 4509	SP-253	Alaska	117
SN 4510	SP-253	Florida	120
SN 3044	SP-206	Germany	123
SN 1380	SP-141	Okinawa	129
SN 1265	SP-112	Alaska	135
SN 0189	SP-007	Germany	142
SN 0183	SP-007	Germany	142
SN 0085	SP-004	North Dakota	143

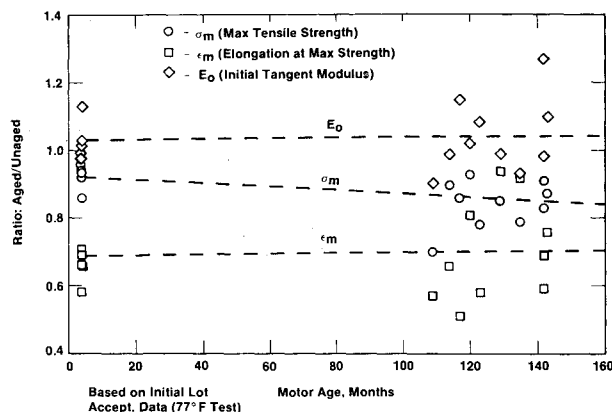
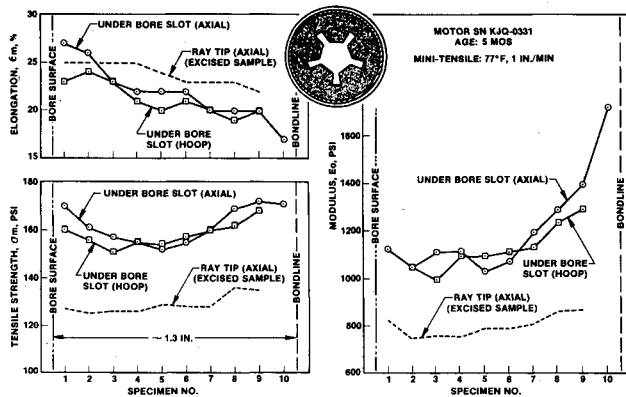


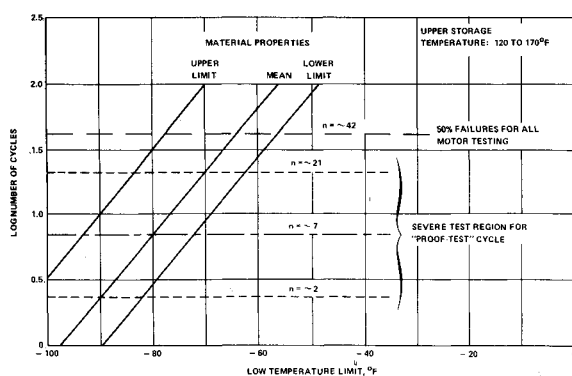
Fig. 2 Grain excised samples.

**Table 2 Comparison of dissected motor results with initial quality assurance data**

Temperature, °F	Motor SN KJQ-0331 <sup>a</sup>			Lot SP-406 Initial Q. A. sample		
	$\sigma_m$	$\epsilon_m$	$E_0$	$\sigma_m$	$\epsilon_m$	$E_0$
-70	—	—	—	517	53	4977
-65	559	34	9374	—	—	—
77	153	20	1231	154	35	846

<sup>a</sup> Age at dissection: 5 months.**Fig. 3 Grain mechanical properties gradients.****Table 3 Grain structural analysis summary**

Design condition	Margins of safety <sup>a</sup>		
	Bond normal stress	Bond shear stress	Inner bore strain
Storage at -40°F	0.55	0.64	-0.05
Storage at -65°F	0.07	0.29	-0.06
Firing at -40°F	—	3.41	0.51

<sup>a</sup> Margin of safety = (allowable/requirement) - 1.**Fig. 4 Design curve for cycle selection (preliminary).**

Both forward and aft ends are unbonded and stress relief is provided at the juncture with the bonded area.

#### Failure Modes Ranking

The first task in the program was a preliminary ranking of potential failure modes. Evaluation of available motor design information, materials properties data, and analysis results indicated that the most likely failure modes for this motor are (in order of decreasing potential):

- 1) Propellant inner bore crack.
- 2) Separation at the propellant-insulation interface.

#### 3) Separation in the propellant near the bondline.

The first mode therefore became the focus for subsequent analytical efforts to design a test cycle which would yield predictable grain failures.

#### Excised Samples

Fifteen motors were provided for the phase I effort. Five were freshly manufactured, while the remaining ten, retrieved from various parts of the world, varied in age from 109 to 143 months (Table 1). Temperature and humidity conditions during storage were unknown. Small propellant samples were excised from the aft grain of each of these motors and mini-tensile and mini-stress relaxation specimens were prepared and tested. Typical mechanical properties data plotted vs motor age are presented in Fig. 2. Note that the values have been normalized with respect to the initial quality assurance (Q.A.) data in order to minimize variability due to batch-to-batch differences.

The propellant material properties in these SEC grains were also unknown, so individual nomographic calibrations had to be made as the material properties were varied. After some familiarity with the properties and the analyses were achieved, it became possible to limit considerations to three distinct groups of data: 1) the average properties for the motors; 2) the best combination of properties, which became the upper limit; and 3) the worst combination, which became the lower limit.

The parameters used in these analyses were derived by direct comparison with data from the dissected motor. First, the data from this motor were carefully evaluated to obtain the desired parameters. Then, the excised sample property data were ranked for the tensile strength,  $\sigma_m$ . The values of the critical strength,  $\sigma_0$ , were then estimated for the remaining motors by direct ratios. Thus, the high, low, and median values were directly and simply obtained. Similar rankings and calculations were made to obtain the remaining parameters.

Since the design curves derived from the above analyses are based upon SEC failure data without a knowledge of the actual material properties involved, there was a degree of uncertainty about the actual placement of these curves. It was therefore expected that further adjustment would be required, based upon the data obtained from the failure and subsequent dissection of the validation motor.

The "proof test" (or validation test) was to be conducted on one full-scale motor containing propellant with properties which place it below the mean design curve. Nevertheless, assuming mean properties and a goal of seven thermal cycles for this test, the design curve in Fig. 4 yielded upper and lower temperature extremes of 170 and -80°F, respectively. Past experience has shown a factor near 3 between the mean and the limits for these testing failures. Thus, the failure of this motor was expected to occur between 2 and 21 thermal cycles.

#### Overtest Cycle Validation

Using the excised sample as a basis, as indicated above, a motor was selected from the youngest age group and subjected to a shock cycle consisting of 16 h at -80°F followed by 8 h at 170°F. After each exposure to low temperature, the

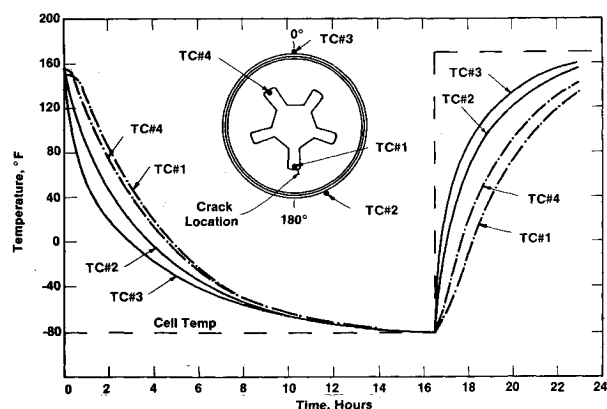


Fig. 5 Typical temperature/time record for motor cycling.

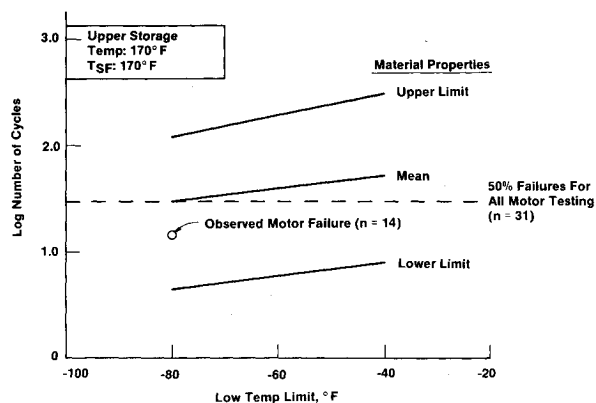


Fig. 6 Revised design curve for cycle selection.

grain inner bore was carefully inspected using a borescope. Inspection after the fourteenth exposure to  $-80^{\circ}\text{F}$  revealed the presence of two small cracks in one of the slots. Post-test radiographic inspection revealed no indication of bond separation in the high-stress areas. The earlier conclusion, based on analysis, that inner bore cracking is the primary failure mode, was therefore substantiated.

Since the grain failed well within the predicted range of 2-21 cycles, the basic overtest cycle was considered to be validated for phase II application. However, comparison of the cycling results for the subject motor with the initial "design curve" for failure prediction (Fig. 4) showed that the failure point for this motor fell well above the predicted mean. Since the motor was selected on the basis of its below-mean mechanical properties (from excised sample data), it became clear that some fine tuning of the analysis was required.

#### Empirical Calibrations

Empirical calibration of the analysis was accomplished by incorporation of actual grain mechanical properties, obtained by post-cycling dissection and test of the validation motor, and the data obtained during the thermal cycling test. Relative to the latter, the thermal responses of the motor were found to be different from those assumed in the nomographic analysis. Accordingly, the thermal conductivity and specific heat values were adjusted to be consistent with those from available reports, then using iterative analyses the optimum heat-transfer coefficients were selected to match the measured inner-bore temperature. The different rates of inner-bore cooling and heating observed in the validation motor are shown in Fig. 5 for the indicated thermocouple locations.

The new viscoelastic/damage analysis yielded a prediction of 17 thermal cycles as compared to the 14 observed. This was considered sufficiently close to require no further calibration

Table 4 Motors selected for overtest cycling

Group	Motor	Lot	Age, months	Cycles-to-failure
A	SN 0293	SP-406	22	>50
	SN 0309	SP-406	22	>50
	SN 0310	SP-406	22	>50
	SN 0319	SP-406	22	>50
	SN 0323	SP-406	22	>50
	SN 0326	SP-406	22	>50
	SN 0333	SP-406	22	>50
	SN 0334	SP-406	22	>50
B	SN 3044	SP-206	127	>13
	SN 4509	SP-253	121	11
	SN 4510	SP-254	121	>13
	SN 5030	SP-264	124	>13
	SN 5081	SP-285	119	>13
	SN 5024	SP-264	119	13
	SN 5320	SP-271	114	10
	SN 5328	SP-271	113	9
C	SN 0085	SP-004	159	> 9
	SN 0163	SP-007	158	9
	SN 0183	SP-007	158	9
	SN 0189	SP-007	158	7
	SN 0442	SP-017	157	> 9
	SN 1265	SP-112	148	7
	SN 1300	SP-112	148	7
	SN 1380	SP-141	145	9

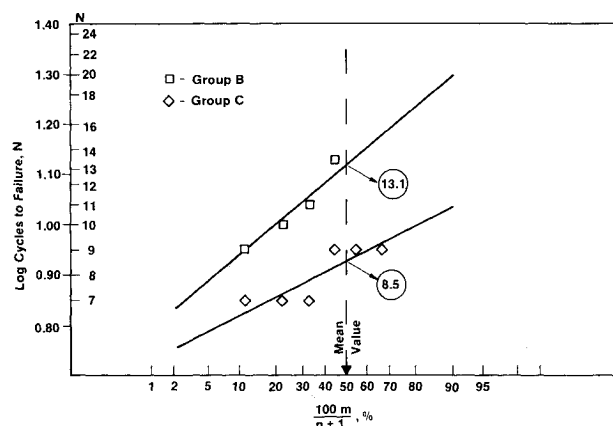


Fig. 7 Estimated distributions for grain failures.

or adjustment in the analysis. Therefore, the refined analyses were used to generate the new design curves for the thermal cycling failure prediction which would apply to the phase II testing, Fig. 6.

Based on the adjusted design curves, it was decided to maintain the same overtest cycle for use in phase II (i.e., 170 to  $-80^{\circ}\text{F}$ ). This cycle preserved the data from the already existing motor test to  $-80^{\circ}\text{F}$ , it yielded a predicted mean number of cycles to failure (31) which was expected to be sufficient for the later studies, and it ensured a conservative limit in case the "actual" mean line should be higher than 31 cycles.

#### Motor Overtests

Fourteen additional motors, similar in origin to the original 15, were provided for test. From the total sample, 24 were selected and divided by age into three groups of eight each. These were designated groups A (youngest), B (middle aged), and C (oldest) as shown in Table 4. Each set of eight was mounted in a special rack to facilitate handling. Two motors in each set were instrumented with internal and external thermocouples.

Table 5 Results of censored sample analysis

Group	Mean log $N$	$\bar{N}$	$\hat{\sigma}(\log N)$
B	1.1185	13.1	0.1425
C	0.9278	8.47	0.0850

Table 6 Estimates of missing values and mean motor ages for groups B and C

Group	Mean motor age, months	Missing values cycles-to-failure, $N$
B	116.8	13.7
		15.1
		16.9
		19.6
C	152.5	9.8
		10.8

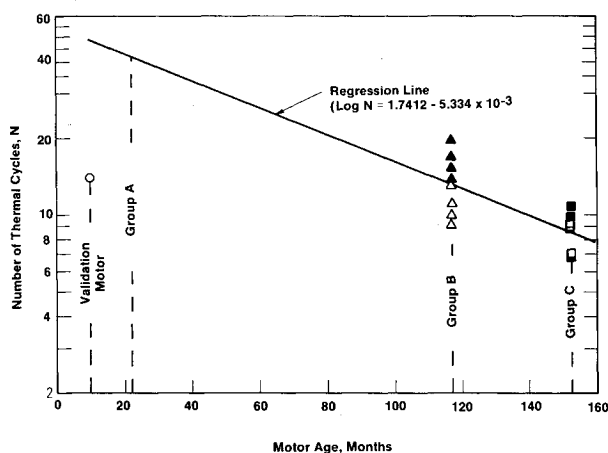


Fig. 8 Semi-log regression analysis of motor failure data.

The three motor sets then were subjected simultaneously to the selected test cycle. In this case, the motors were exposed to each temperature extreme for a minimum of 22 h. Each motor was inspected by borescope after each low-temperature exposure. Thermocouple outputs of the instrumented motors were monitored continuously.

The results of the overtest cycling are summarized in Table 4. As indicated, six failures occurred in the oldest age group (C), four in the middle age group (B), and none in the youngest group (A). The 50% failure target was exceeded with group C because the motors failed in groups of three each on the seventh and ninth cycles. The lack of failures in group A was unexpected, but subsequent motor dissection showed evidence of severe hydrolytic degradation of the propellant, probably due to "breathing" in of humid air during the numerous thermal cycles to which the motor was exposed. Based on the above observation, it was concluded that the softening, and associated increased strain capability, occurred before the critical number of cycles was reached, and thereby prevented grain cracking.

#### Motor Static Firing

Ten motors which survived overtest cycling without failure were selected for static firing at  $-40^{\circ}\text{F}$ . Comparison of the ballistic performance of the ten motors with specification requirements and with the results of a Navy surveillance program showed all motors to be within normal limits. From these results, it was concluded that if the grain is intact prior to firing, the motor will perform normally regardless of age or level of mechanical damage.

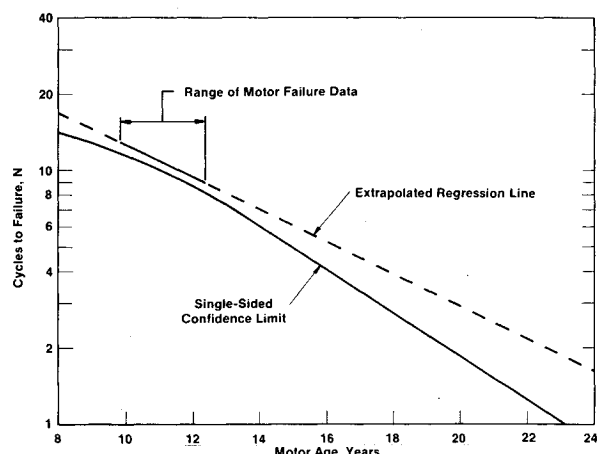


Fig. 9 Single-sided confidence limit for the "true" line of regression.

#### Data Analysis

An overall review of the motor test results indicates three major problems which make an age-life prediction for this specific motor particularly difficult. First, the motors are biased with respect to the lots from which they were chosen. All group A motors contained propellant from the same mix, while five of the six motors which failed in group C represented only two propellant mixes, and two of the four failed motors in group B were cast from the same mix. Second, no verifiable failures were obtained from group A. The single data point from the validation test, at 10 months, is of very limited value since the motor was selected on the expectation that it would be one of the earliest failures in the group A tests. Without confirmatory group A failures, it is uncertain whether this test result is an outlier or a representative result that would have been among the earliest of the motor failures. Finally, the age difference between groups B and C is very small relative to the total age spread for all of the motors. Because of these problems, it is not possible to define accurately the shape of the trend line which best represents the aging behavior.

In view of the limitations noted, the following data analysis is provided for illustrative purposes only. An arbitrarily selected aging trend line is assumed which is based upon previous observations that propellant cumulative damage failures (of which motor thermal cycling failures are examples) follow a log-normal statistical distribution. Thus, the logarithm of the number of thermal cycles-to-failure,  $N$ , becomes the dependent variable, while the selected regression relation becomes

$$\log N = a - bA \quad (1)$$

where  $A$  is the motor age in months and  $a$ ,  $b$  are regression coefficients.

The overtest cycling had followed a censored sampling plan where all the motors in each group were subjected to the test cycle at the same time, the test being terminated after half of them had failed (called the point of censorship or truncation point). This censoring technique permits treatment of each motor failure as if it were part of the overall sample, yet the unfailed motors can be set aside for other testing purposes. The basic statistical parameters, the mean and standard deviation, may be estimated by various methods of order statistics.<sup>2,3</sup> These methods require that the entire motor sample (of each group) be a random selection from a normally distributed population. In this case, the logarithms of the number of thermal cycles-to-failure would be normally distributed. Accepting the latter assumptions, the censored sample test results for groups B and C were plotted on a log-probability scale and the means and standard deviations determined by least-squares analysis (Fig. 7). The key values from the analysis are given in Table 5.

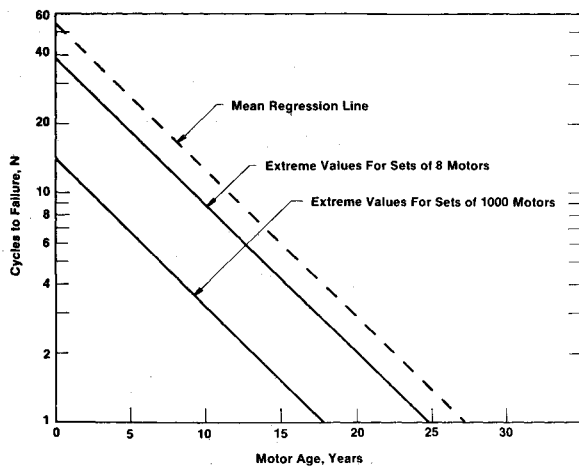


Fig. 10 Extreme value projections.

Table 7 Age-life projections

Motor sample size, $n$	Estimated age-life, yr	
	Linear projection	90% confidence limit
1	27	23
8	25	21
1000	18	10

The mean variance for  $\log N$  obtained from this analysis gave the average  $\sigma$  of 0.1174. This is lower than previously observed values, which typically range from 0.15 to 0.30.

For purposes of the regression analysis, it was necessary to make estimates of the missing data from each group. The methods given in Refs. 4 and 5 were used to obtain these values, which are listed in Table 6. Also included in Table 6 are the group mean ages.

The regression line derived from these motor failure data is shown in Fig. 8, which includes the individual results and estimated missing values for groups B and C. The regression relationship was determined to be

$$\log N = 1.7412 - 5.334 \times 10^{-3} A \quad (2)$$

or

$$N = 55.1 \times 0.9878^A \quad (3)$$

A line of regression is an estimate of average, or central, tendency. Because of the inherent variability of the materials and the testing process, the estimated average line can only approximate the true one. It is customary, therefore, to place limit lines on both sides of the line of regression within which the average of a small sample may be expected to lie with some selected degree of confidence. The usual practice for service life projections is to represent the real material capability by the lower limit line and estimate motor age-out as the intersection of this line with a specification limit or arbitrary motor requirement. Unfortunately, this method does not permit the determination of when the first few motors in a given population will not perform to specification. Since the latter should be of primary interest in any age-out prediction, the approach selected here involves the application of single-sided confidence limits to estimates of the extreme values for motor behavior.

The single-sided confidence limit falls about 23% closer to the regression line than does the two-sided limit for the 90% level of confidence. As shown in Fig. 9, this single-sided limit defines, at 90% confidence, the minimum placement for the true regression or, for the purposes of this evaluation, the age at which the minimum grain structural performance would be expected.

The approach used for the determination of the extreme values followed that developed by Freudenthal.<sup>6</sup> Some slight

modifications to the relationships were made to yield predictions of the number of thermal cycles,  $N_m$ , to produce the  $m$ th failure in a motor sample of size  $n$ . Combining this with a relationship for the mean number of thermal cycles-to-failure,  $\bar{N}$ , for log-normal statistical distribution gave

$$\frac{N_m}{\bar{N}} = \left[ -\ln \left( 1 - \frac{m}{n+1} \right) \right] / \alpha \Gamma \left( 1 + \frac{1}{\alpha} \right) \quad (4)$$

where  $\alpha$  is derived from the estimated standard error  $\hat{\sigma}(\log N)$  using the following relationship:

$$\alpha = (\pi/5.461) [1/\hat{\sigma}(\log N)] \quad (5)$$

The previously calculated value for  $\hat{\sigma}(\log N)$ , 0.1174, was used to obtain  $\alpha = 4.746$ . Then, setting  $m = 1$  and  $n = 8$  and 1000 in Eq. (4) gave the desired values for  $N_1/\bar{N}$ , the relative number of cycles to first failure. These ratios are 0.6961 and 0.2548 for sample sizes of 8 and 1000 motors, respectively. Multiplying the regression line by these values yields the two extreme value lines given in Fig. 10.

At this point a more rigorous analysis would require that a further adjustment of the extreme value lines be made to account for the difference, in a cumulative damage sense, between the overtest cycle used and typical real-life motor exposures over a period of 1 yr. However, for the purposes of this example the criterion for age-out has been arbitrarily defined as one overtest cycle. Extrapolation of the extreme value lines to this point yields the age-life projections given in Table 7. Also included are the values obtained by applying the single-sided 90% confidence limits to each of the extrapolations.

It is recognized that it is always dangerous to extrapolate too far beyond the limits of the data from which a trend line has been derived. As indicated by the dashed line in Figs. 9 and 10, the questionable area of extrapolation in this case is sizeable. However, the nature of service life prediction requires this type of extrapolation, so the risk must be minimized by ensuring that the data which are used are the most representative and cover the broadest range possible. In addition, periodic updates of the prediction using the results of additional tests of motors selected from the oldest age group deployed in the field are recommended.

## Conclusions

The results of the program discussed in this paper have demonstrated that the prediction of the age-out of air-launched motors, using a technique based on chemical/structural overtesting of aged full-scale motors, is feasible. The key is the ability to fail the motors with a reasonable test cycle. However, once this requirement has been met it becomes extremely important that the motors selected for test represent an unbiased, random sample of the population, and that an adequate age spread exists between the motor sets.

## Acknowledgments

This work was sponsored by the Air Force Rocket Propulsion Laboratory, Research and Technology Division, under Contract F04611-79-C-0035. The encouragement and support given by Ross Stacer, Project Manager, is deeply appreciated.

## References

- 1 Bills, K. W. Jr., "Structural Design Nomograph for Thermal Cycling of Tactical Rocket Propellants," NWC Tech. Memo 3365, Dec. 1977.
- 2 Gupta, A. K., *Biometrika*, Vol. 39, 1952, pp. 260-273.
- 3 Sarhan, A. E. and Greenberg, B. G., *Annals of Mathematical Statistics*, Vol. 27, 1956, pp. 427-451.
- 4 Wilkinson, G. N., *Biometrics*, Vol. 14, 1958, p. 257.
- 5 Biggers, J. D., *Biometrika*, Vol. 46, 1959, p. 91.
- 6 Freudenthal, A. M., "The Expected Time for First Failure," AFML-TR-66-37, Feb. 1966.